International Journal of Physical Modelling in Geotechnics
Volume 15 Issue 1

Use of Ricker motions as an alternative to pushover testing
Loli, Knappett, Anastasopoulos and Brown

International Journal of Physical Modelling in Geotechnics, 2015, **15**(1), 44–55
http://dx.doi.org/10.1680/ijpmg.14.00009
Paper 1400009
Received 19/04/2014 Accepted 18/12/2014
Published online 26/02/2015
Keywords: geotechnical engineering/research & development/seismic engineering

Use of Ricker motions as an alternative to pushover testing

Marianna Loli Dipl., MSc
National Technical University of Athens, Zografou, Athens, Greece

Jonathan Adam Knappett MA, MEng, PhD
University of Dundee, Dundee, UK

Ioannis Anastasopoulos Dipl., MSc, PhD
University of Dundee, Dundee, UK

Michael John Brown BEng (Hons), PhD
University of Dundee, Dundee, UK

When undertaking centrifuge studies on seismic soil–structure interaction, it is useful to be able to define the pseudo-static 'pushover' response of the structure. Normally, this requires separate centrifuge experiments with horizontal actuators. This paper describes an alternative procedure, using Ricker ground motions to obtain the pushover response, thereby allowing both this and the response to seismic shaking to be determined using a centrifuge-mounted shaker. The paper presents an application of this technique to a 1:50 scale model bridge pier with two different shallow foundations, as part of a study on seismic protection using rocking isolation. The moment–rotation ('backbone') behaviour of the footings was accurately determined in the centrifuge to large rotations, as verified through independent three-dimensional dynamic non-linear finite-element modelling. Ricker wavelet ground motions are therefore shown to be a useful tool for the identification of pushover response without requiring additional actuators. Furthermore, a simplified analytical methodology is developed, which allows one to predict the maximum foundation rotation induced by a specific Ricker pulse. This methodology may be useful in predicting the characteristics (frequency and acceleration magnitude) of the Ricker pulse required to describe the pushover response of any (practically) rigid oscillator supported on shallow foundations.

Notation

A	acceleration
a_{deck}	deck acceleration
a_{E}	acceleration at the model base (excitation)
a_{FF}	free-field acceleration
B	foundation width
D_{r}	relative density of the soil
d	displacement
E	Young's modulus
FS_{E}	factor of safety in seismic loading
FS_{V}	factor of safety in vertical loading
f_{E}	excitation frequency
H	pier height
M	moment load
m_{deck}	deck mass
N	vertical load
Q	horizontal load
S_{a}	spectral acceleration
S_{d}	spectral displacement
T	period
t	time
z	depth
γ	unit weight
δ	horizontal displacement
δ_{F}	horizontal displacement due to column bending
δ_{R}	horizontal displacement due to foundation rotation
δ_{res}	residual horizontal displacement
δ_{s}	horizontal displacement due to foundation sliding
δ_{tot}	total horizontal displacement
θ	rotation
θ_{c}	critical rotation causing overturning on a rigid base
θ_{uplift}	rotation causing onset of uplifting
σ_{v}	total vertical stress
ϕ	soil friction angle
ϕ'_{peak}	peak friction angle
ϕ'_{crit}	critical state friction angle

1. Introduction

The understanding of seismic soil–structure interaction has been developed to the point where it is possible to use the ductile characteristics of foundation rocking to protect structures from more catastrophic brittle forms of failure (e.g. Anastasopoulos *et al*., 2010; Gajan and Kutter, 2008; Gajan *et al*., 2005; Gelagoti *et al*., 2012; Paolucci *et al*., 2007; Pecker, 2005). The key concept underpinning this design approach is that the moment capacity of the foundation is lower than that which causes damage to the supported column or pier, resulting in shallow foundations that are smaller than those produced by conventional design approaches (aiming to prevent inelastic foundation response). This relies on adequate characterisation of the moment–rotation pushover response of the system.

A recent collaborative study has been undertaken between the National Technical University of Athens and the University of Dundee. This study, reported by Loli *et al*. (2014), focused on the use of rocking isolation seismically to protect Eurocode 2- (CEN, 2005) and Eurocode 8- (CEN, 2004) compliant reinforced-concrete bridge structures. Figure 1 shows the conceptual prototype problem, where a 10·75 m tall bridge pier, carrying the dead load of the deck (300 Mg), is founded on a shallow, 10 m thick layer of medium density sand (relative density, $D_r = 60\%$) with a square ($B \times B$) footing. This was structurally designed to resist a ground motion of 0·2$\boldsymbol{g}$ to Eurocode 8 (CEN, 2004) design principles, as outlined by Loli *et al*. (2014). Two models were tested, the only difference between them being the foundation dimensions, with the aim of comparing two different approaches with aseismic foundation design as summarised in Table 1. The larger footing ($B = 7{\cdot}5$ m) followed the current code provisions ensuring minimal displacements of the soil–foundation interface under the design earthquake – that is, the factor of safety against seismic loading (FS_E) is greater than 1. The alternative design ($B = 4$ m) promoted the newly introduced concept of foundation rocking isolation with $FS_E < 1$.

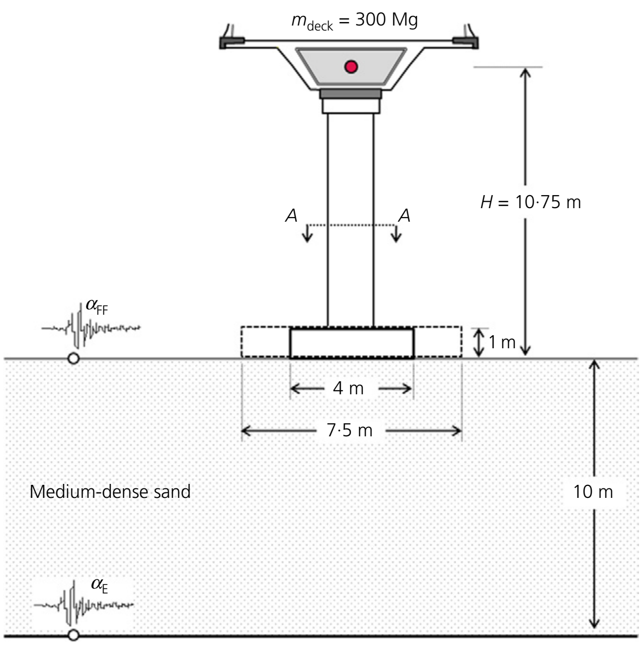

Figure 1. Schematic diagram of the problem considered: bridge pier on a shallow foundation considering two different sizes/designs

Property	Large footing	Small footing
Breadth: m	7·5	4·0
Vertical load: MN	4·9	4·0
Design shear load: MN	1·0	0·7
Design moment: MN m	10·6	7·6
FS_V: static	18	3·5
FS_V: seismic	1·7	0·6

Table 1. Footing designs considered in this study (all values at prototype scale)

During this study, the model bridge piers were realistically modelled using new scale-model reinforced concrete ('model-RC') developed at the University of Dundee and described by Knappett *et al.* (2010, 2011) and Al-Defae and Knappett (2014a, 2014b). The structural design and validation of the properties of the model piers are described by Loli *et al*. (2014). In addition to testing the response of these damageable structures under historical ground motions, it was necessary to check the moment–rotation response of the foundation designs, to ensure that the structural moment capacity fell between the moment capacities of the two foundations that were associated with $FS_E < 1$. The yield surfaces for the two foundations in N–Q–M space (N = vertical load, Q = horizontal load, M = moment) for these foundations on the test soil (dry sand, properties given below) were estimated after Butterfield and Gottardi (1994) and are shown in Figure 2. Two yield surfaces are shown in each case with the outer representing peak friction angle conditions (ϕ'_{peak}) and the inner based on the critical state friction angle for the soil (ϕ'_{crit}). It can be seen that the combination of loads acting on the structure lies between the yield surfaces implying that the small foundation will isolate the structure through rocking, while the larger one will not.

Determining the capacity of the footings posed a significant challenge as the timescale of the project meant that producing different centrifuge set-ups using horizontal actuators would not have been achievable. Therefore, it was decided to investigate the possibility of using a carefully selected dynamic ground motion to produce a 'virtual pushover' of the structure–foundation model. This set of tests was conducted on a geometrically identical pier model, but with the model RC piers replaced with elastic columns, made of aluminium, to supress concrete failure and focus on foundation response. Initially, it was intended to match these to the initial linear elastic bending stiffness of the model-RC columns (=10·76 GN m^2 at

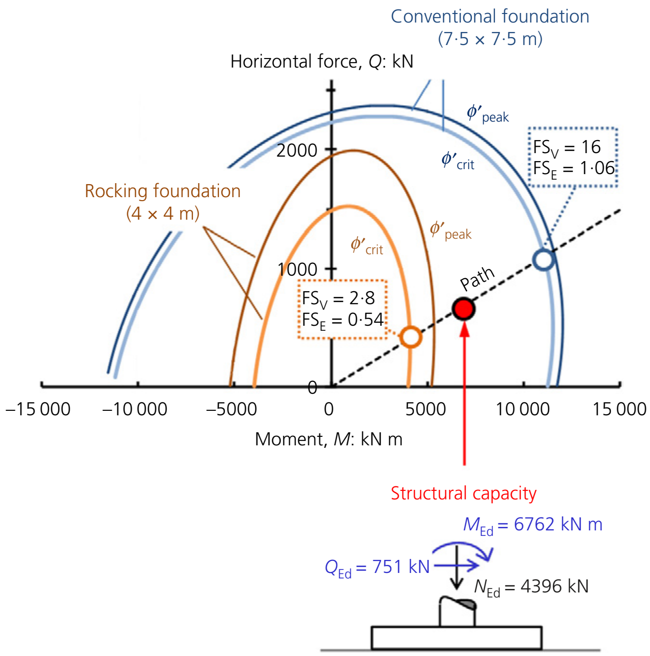

Figure 2. Foundation yield surfaces along with structural capacity shown for comparison

prototype scale); however, preliminary numerical modelling (described later) indicated that using a stiffer structure, approximately 2·7 times stiffer in bending, would suppress flexural oscillations and ensure that the dynamic response of the pier be dominated by foundation rocking. Although this leads to unrealistic modelling of the bridge pier stiffness characteristics, promoting foundation rocking in this way was essential in facilitating the approximation of the foundation moment capacity and moment–rotation backbone curve through shaking, which was the main objective of this work.

2. Ricker wavelets

When using a ground motion to simulate a pushover test, possible excitation alternatives include a step-type motion or various types of pulse input, including single sine pulses, 'fling' pulses and Ricker wavelets. All of these are capable of producing a peak spectral displacement of significant magnitude to induce substantial rocking, provided that the dynamic characteristics of the structural system are tuned to have a suitably long natural period. Preliminary numerical modelling was conducted, as described in the following section, to evaluate these different possibilities. Thanks to their single characteristic pulse, Ricker wavelets were found to be most efficient in accurately approximating the monotonic static response. It was observed that they are generally able to mobilise a larger amount of the rotation capacity than the other pulse types, while also having the advantage that the earthquake actuator slip table automatically comes back to rest in its original starting position, without having a permanent displacement offset. This removes the need to re-centre the table before subsequent motions.

In total, 15 different Ricker wavelets were considered involving three different dominant frequencies, $f_E = 2$, 1 and 0·5 Hz, scaled to peak accelerations of 0·2g, 0·4g, 0·6g, 0·8g and 1·0g. Figure 3 shows the acceleration (α) time histories of the Ricker wavelets used in the numerical analysis and the respective elastic displacement spectra (S_d) for peak ground acceleration (PGA) = 1·0g.

3. Numerical modelling

3.1 Finite-element discretisation

Three-dimensional (3D) dynamic non-linear finite-element (FE) modelling was conducted using Abaqus to investigate the behaviour of the bridge structure and underlying soil under different ground motions for simulating pushover. These analyses also serve the function of predicting the centrifuge test results which will be described later in the paper. Figure 4 displays the sufficiently refined FE mesh and indicates the main features of the numerical model. The geometry is that of the centrifuge model at prototype scale. The deck and the footing were simulated using eight-noded hexahedral continuum elements, attributed to the elastic properties of steel and aluminium, respectively. The same element type, incorporating non-linear material response, was used to model the sand layer. The 1·5 m × 1·5 m square section pier was simulated with 3D elastic beam elements assigned the geometric and elastic stiffness properties of the aluminium section used in the centrifuge tests ($E = 70$ GPa, $\gamma = 26$ kN/m^3).

Given the relatively high position of the deck mass, second-order (P–δ) effects are of great importance and were therefore taken into account. The lateral boundaries of the model are free to move horizontally and were assigned suitable stiffness properties so as to reproduce realistically the response of the equivalent shear beam (ESB) flexible wall container used in the centrifuge and described by Bertalot (2012). Taking advantage of symmetry on the plane that crosses the foundation midpoint in the direction of shaking allowed simulation of only half of the full 3D model, achieving greater computational efficiency.

3.2 Soil properties

The non-linear behaviour of medium density silica sand (relative density $D_r = 60\%$, unit weight $\gamma = 15{\cdot}5$ kN/m^3), which was used in the experiments, was simulated using a simplified kinematic hardening model with Von Mises failure criterion and associated flow rule, modified appropriately to reproduce

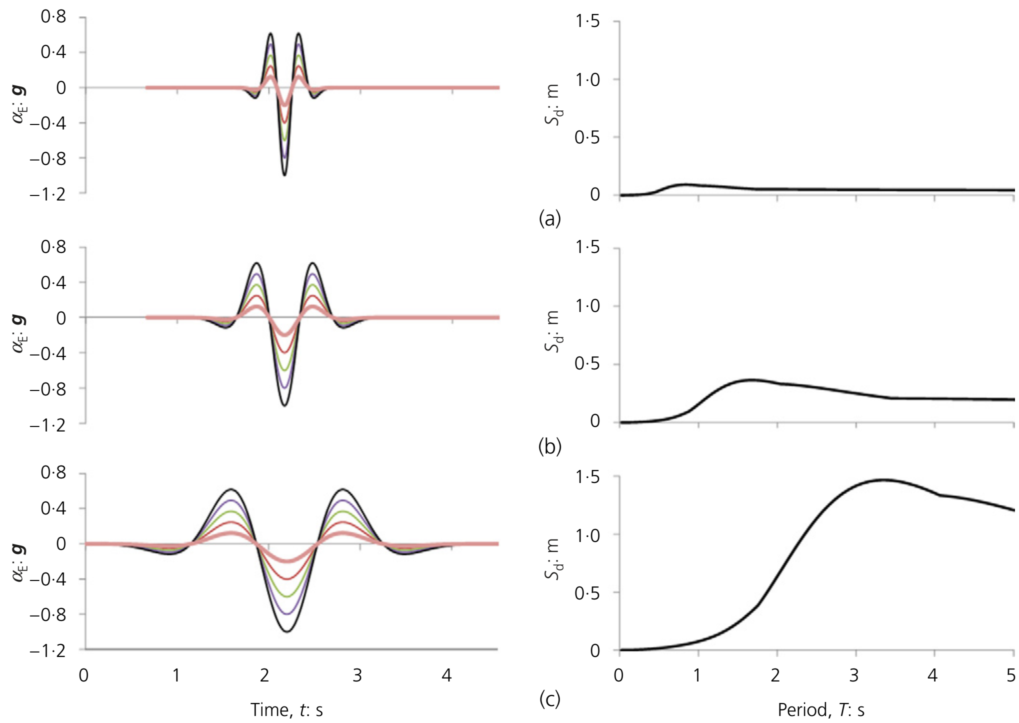

Figure 3. Acceleration time histories and elastic ($\xi = 5\%$) displacement response spectra (shown only for PGA = 1**g**) for the Ricker wavelets: (a) $f_E = 2$ Hz; (b) $f_E = 1$ Hz; and (c) $f_E = 0{\cdot}5$ Hz

the pressure-dependent behaviour of sands as well as that of clays. Details of this model can be found in the paper by Anastasopoulos *et al.* (2011). Despite its lack of generality, the model has been shown to capture satisfactorily the non-linear response of a shallow foundation on compliant soil

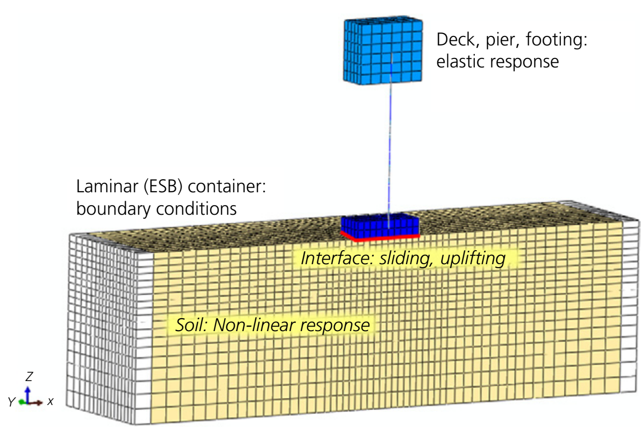

Figure 4. Details of the 3D FE simulation of the centrifuge model

(Anastasopoulos *et al.*, 2011). Moreover, in an attempt to provide a more realistic representation of the pressure-dependent sand behaviour, a user subroutine was encoded to provide variation of strength and stiffness properties with depth according to the relationships ϕ–σ_v and E–z shown in Figure 5. The data in the figure are based on basic characterisation testing for the sand used in the centrifuge model tests, which may be found in the paper by Al-Defae *et al.* (2013). The soil–foundation interface was modelled using contact elements, which allow sliding and uplifting to take place while being governed by a hard-contact law and Coulomb's friction law in the normal and tangential directions, respectively.

3.3 Response under Ricker excitation

A series of dynamic analyses was conducted in the time domain, wherein the model base was excited by a variety of idealised pulses (namely, sine, fling and Ricker pulses). Their intensity characteristics, such as peak acceleration and frequency, were parametrically varied in order to determine the pulse most appropriate to use in the centrifuge tests. Yet, this selection of excitation time histories was limited by a requirement for maximum displacement of less than 0·25 m, which is

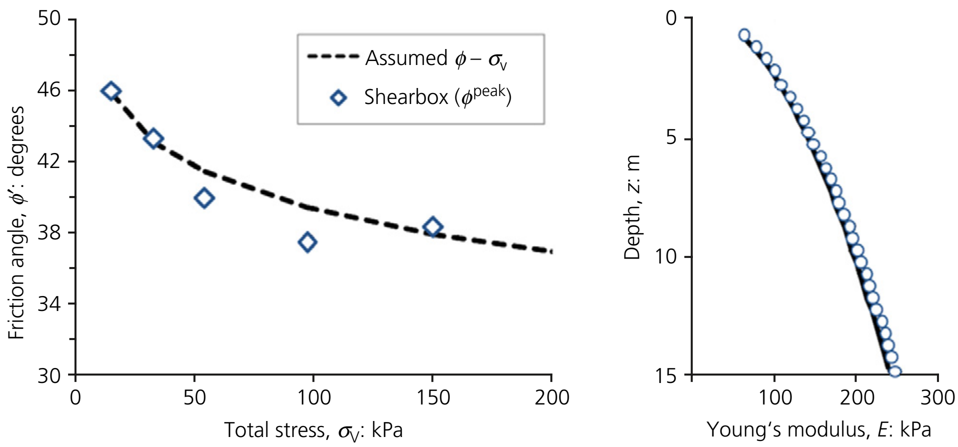

Figure 5. Stress- and depth-dependent soil properties used in the FE model

the capacity of the shaking table in prototype scale. Figures 6 (a) to 6(d) show acceleration and displacement time histories of four of the pulses used in the numerical study. It may be observed that in all cases the input displacement does not exceed the limit of 0·25 m. Given this restriction, the Ricker pulse appears to have two significant advantages: it ensures greater spectral response over a wide range of periods (Figure 6(e)); and it gives zero permanent displacement facilitating the simulation of the excitation time history with a shaking table.

Figure 7 shows the numerically computed dynamic response of the two foundations in the moment–rotation plane under excitation with 1 and 0·5 Hz Ricker pulses (for two different PGA magnitudes). This is compared with the monotonic backbone curves calculated through numerical analysis of the same systems under horizontal pushover loading applied statically at the centre of mass of the deck. It is important to note that the calculated ultimate moment capacities are in good agreement with theoretical estimates (refer to Figure 2).

Strongly non-linear behaviour may be identified in the shape of the single significant loop produced during each excitation pulse, this being presumably more pronounced with increasing excitation acceleration and/or dominant period. Having substantially greater displacement spectral ordinates over the entire range of periods (see Figure 3), the 0·5 Hz Ricker pulses naturally cause both foundations to respond well within the non-linear regime, pushing them to much larger rotation amplitudes in comparison with shaking with the 1 Hz Ricker pulse. Excessive material non-linearity is manifested especially in the case of the smaller foundation leading to some considerable permanent rotation for both the PGA cases shown. On the other hand, the response of the larger foundation is mainly associated with uplifting (loss of contact with the supporting soil), rather than soil yielding, and hence the $M-\theta$ loop resembles the well-known characteristic S-shape. Most importantly, in both cases the dynamic loops approximated the backbone curves satisfactorily indicating that Ricker pulses, especially those having a substantially large dominant period, may be used in centrifuge tests to measure indirectly the ultimate lateral load foundation capacity.

4. Centrifuge modelling

4.1 Model set-up

Two dynamic centrifuge tests were conducted on 1:50 scale physical models of the bridge pier system, with identical superstructural properties, but with different foundations ($B = 7{\cdot}5$ and 4·0 m). In each case, the structures were placed on dry fine Congleton silica sand (HST95, $\gamma_{max} = 1758$ kg/m^3, $\gamma_{min} =$ 1459 kg/m^3, $D_{60} = 0{\cdot}14$ mm, $D_{10} = 0{\cdot}10$ mm, critical state friction angle $\phi'_{crit} = 32°$), prepared uniformly by air pluviation to a relative density, $D_r \approx 60\%$. The deposit of sand was 200 mm deep (i.e. 10 m at prototype scale) and was prepared within the equivalent shear beam (ESB) container described by Bertalot (2012) to minimise dynamic boundary effects. Instrumentation consisted of 13 type ADXL78 micro electromechanical system (MEMS) accelerometers (±70***g*** range) and linear variable differential transformers (LVDTs) as shown in Figure 8. The models were loaded onto the Actidyn Q67-2 servo-hydraulic earthquake simulator (EQS: see Bertalot *et al.* (2012) and Brennan *et al.* (2014) for a detailed description). Due to the limitations in displacement capacity of the EQS, it was not possible to reproduce the desired 0·5 Hz Ricker pulses and therefore the 1 Hz Ricker wavelet with PGA = 0·6***g*** was used as excitation in both tests. All subsequent results in this paper will be given at prototype scale at 50***g***.

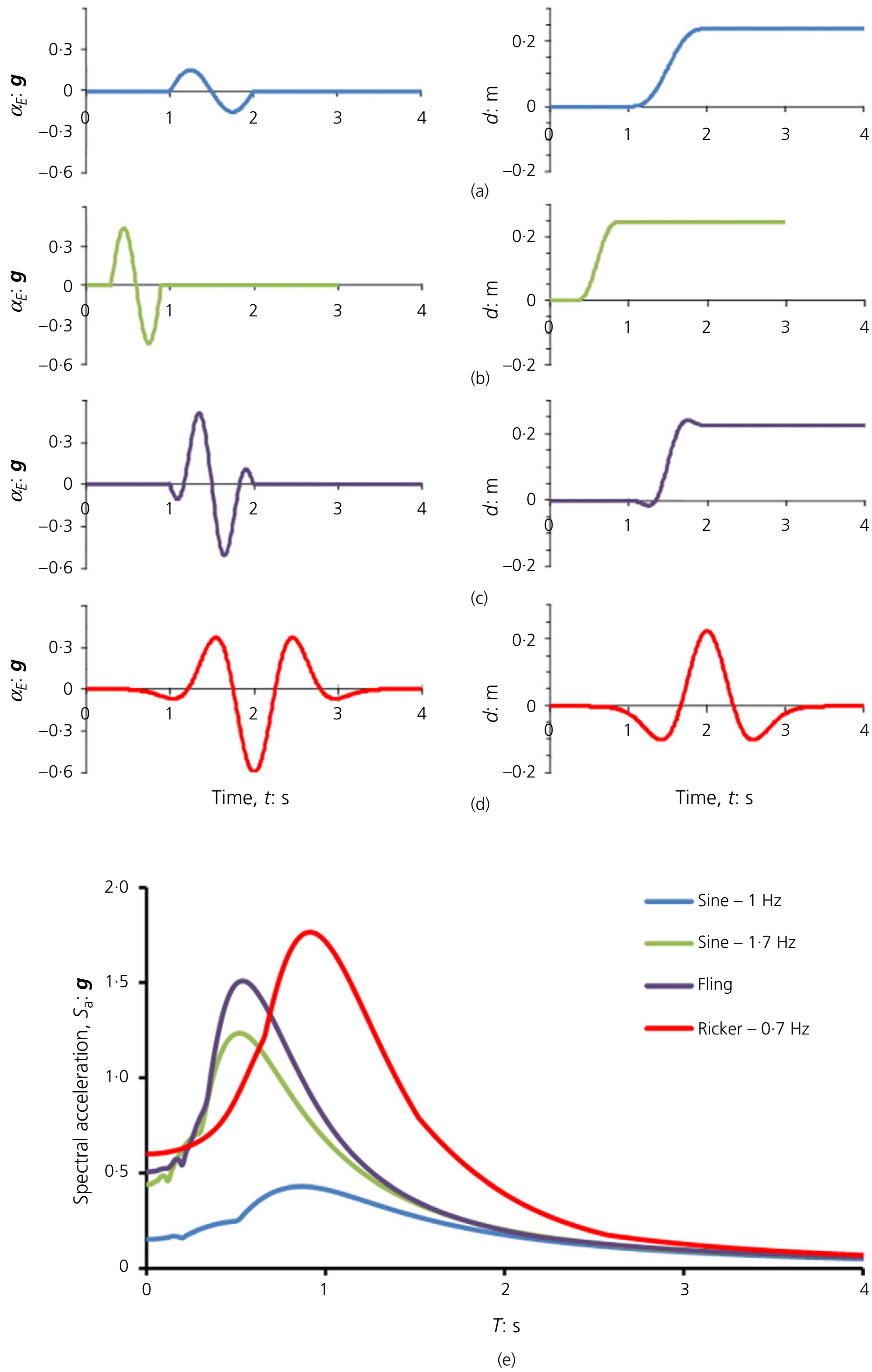

Figure 6. Acceleration and displacement time histories of the idealised pulses used as bedrock excitations: (a) sine 1 Hz, 0·2***g***; (b) sine 1·7 Hz, 0·44***g***; (c) fling 1 Hz, 0·5***g***; (d) Ricker 0·7 Hz, 0·6***g***; (e) acceleration response spectra of the bedrock excitation pulses ($\xi = 5\%$)

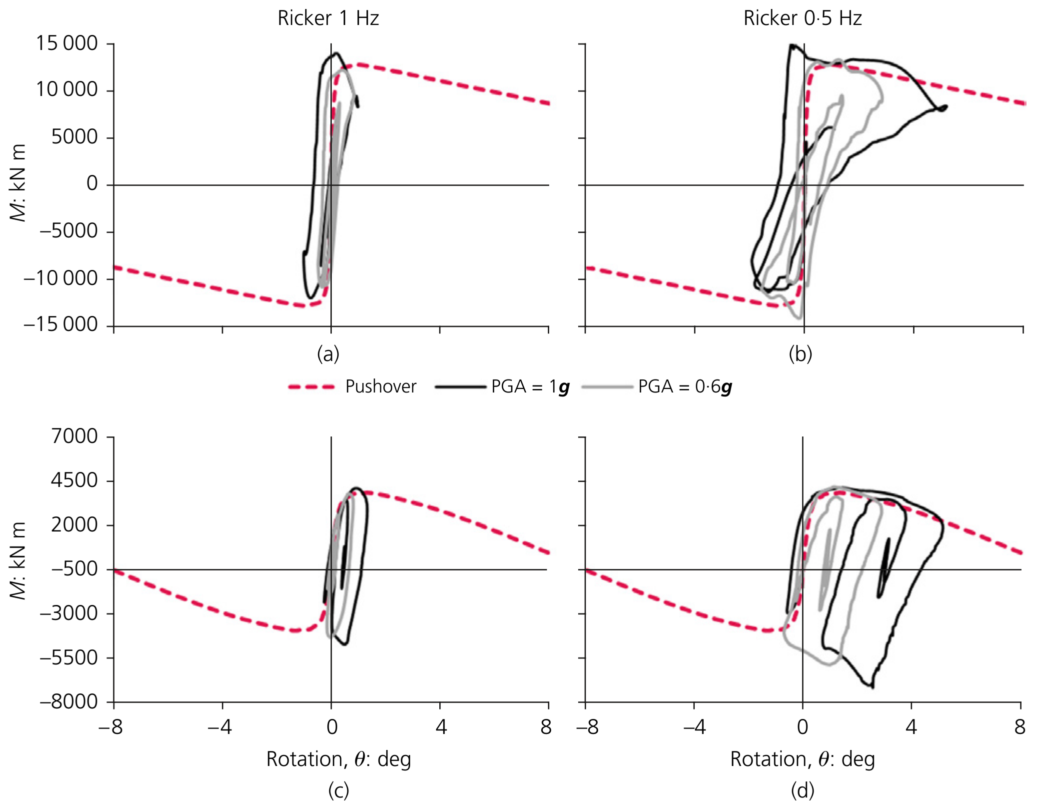

Figure 7. Numerically computed foundation moment–rotation loops compared with monotonic pushover response for the large foundation model with (a) 1 Hz and (b) 0·5 Hz Ricker wavelets; and the small foundation model with (c) 1 Hz and (d) 0·5 Hz Ricker wavelets for two different amplitudes (PGA = 0·6***g*** and 1·0***g***)

4.2 Motion replication and dynamic response

Figure 9 shows the accelerations measured at the centre of mass of the deck in each of the two models – these were determined as the average of the instruments at the top and bottom of the deck mass as shown in Figure 8. The demand motion, slip table motion and free-field ground motion (top-most instrument on the right-hand column of buried accelerometers in Figure 8) are also plotted. It can be seen that the EQS faithfully reproduced the input motion, and that there was some free-field amplification within the soil.

Figure 10 shows the lateral drift of the deck of the bridge, the total component δ_{tot} (due to sliding, δ_s, flexural displacement of the pier, δ_F and rotation, δ_R); δ_{res} represents the residual value of δ_{tot} (i.e. the final unrecovered displacement). Due to a failure in one of the LVDTs recording the vertical foundation movement, it was not possible to measure δ_R independently for the case of the small foundation. However, geometric and physical properties of the pier standing on the small foundation (slenderness, relatively low factor of safety in vertical loading and significantly lower foundation rotational stiffness in comparison to the large foundation) suggest that rocking motion would sufficiently dominate the other two possible modes of response (i.e. sliding would be significant for a less slender oscillator and flexural bending was intentionally suppressed here by the significantly high column stiffness) so as to assume $\delta_R \approx \delta_{tot}$. This dominant role of rocking oscillations, especially in the case of the small foundation, was confirmed by the results of the numerical analysis.

5. Pushover response

The values of δ_R were used with pier height h to determine the rigid body foundation rotation

1. $$\theta = \sin^{-1}\left(\frac{\delta_R}{h}\right)$$

The moment at the bottom of the pier (which is the same as the moment input to the foundation) was determined using the

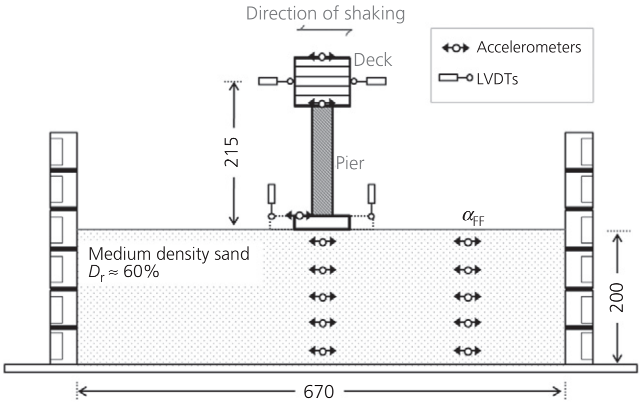

Figure 8. Experimental setup for centrifuge testing (small foundation shown; large foundation indicated by dashed line (bottom of the pier); all dimensions in mm)

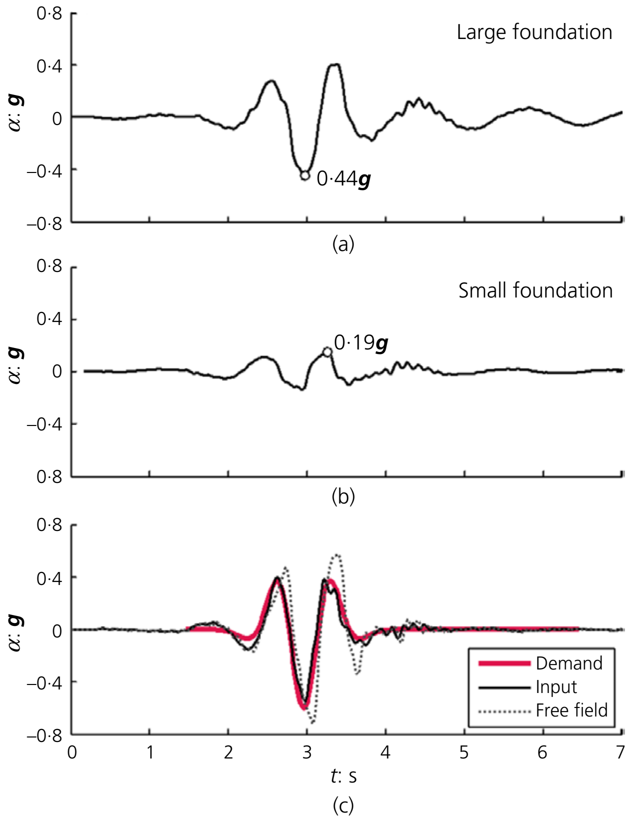

Figure 9. Accelerations recorded during centrifuge tests: (a) deck acceleration, large foundation; (b) deck acceleration, small foundation; (c) demand, input and free-field motions

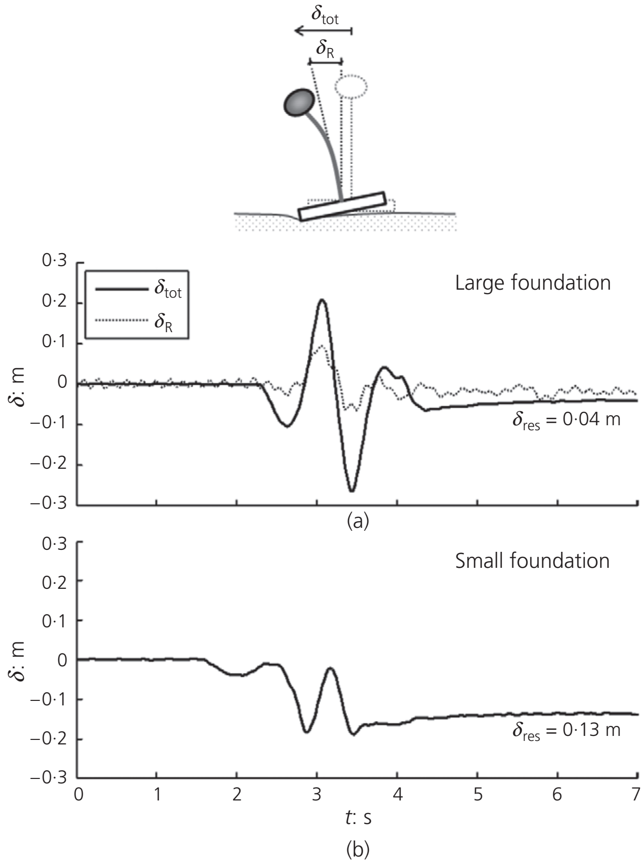

Figure 10. Deck drift time histories recorded during centrifuge tests for table excitation with Ricker 1 Hz PGA = 0·6**g**: (a) bridge pier on large foundation and (b) bridge pier on small foundation

accelerometer data at the deck (a_{deck}), recognising that the system is a cantilever

2. $M = m_{deck} a_{deck} h$

In Equation 2, m_{deck} represents the mass at the top of the pier. Figure 11 shows the moment–rotation loops derived for the centrifuge data, and also plots the static pushover curve determined from the finite-element method (FEM). Considering the small foundation first, it is clear that for the case of foundations exhibiting substantial rocking, even a single Ricker pulse was sufficient to mobilise the moment capacity well into the non-linear (large rotation) domain. The match to the numerical backbone curve is very satisfactory, and suggests that this could be determined from the centrifuge test data by fitting an envelope around the centrifuge data within the positive quadrant (Figure 11).

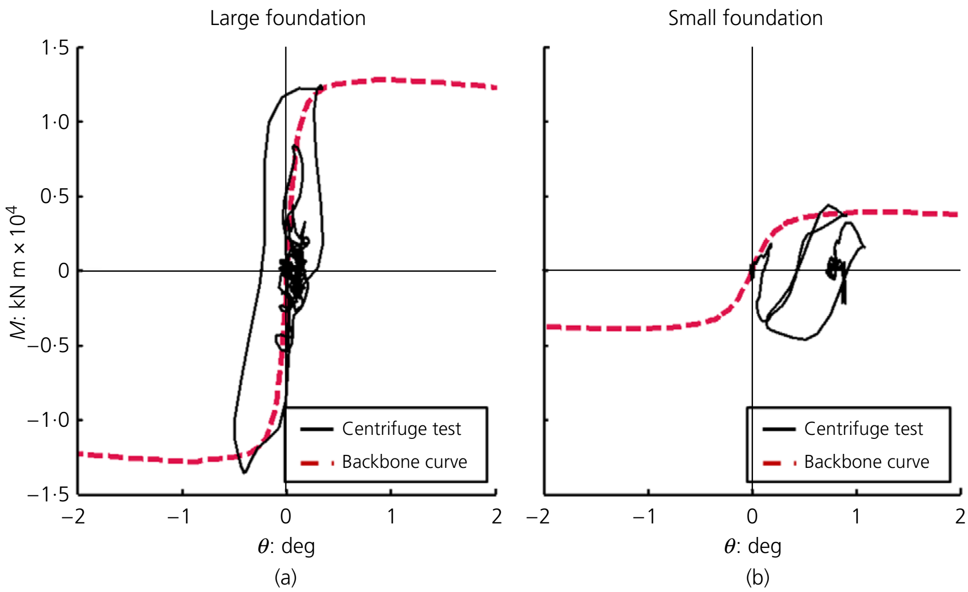

Figure 11. Foundation moment–rotation behaviour determined from centrifuge tests, compared with monotonic pushover ('backbone') curves from FE model: (a) large foundation and (b) small foundation

In the case of the large foundation, much lower rotations were mobilised. This is due to the fact that the large foundation has significantly greater stiffness and capacity, thereby leading the pier to respond primarily through swaying and secondarily through rocking (as indicated by Figure 10(a), where δ_R is a smaller proportion of the total deck drift, δ_{tot}) as opposed to the small foundation pier, which responds primarily through rocking. Nevertheless, the maximum and minimum points of the loops agree well with the backbone curve. In this case, it is suggested that centrifuge testing with a single Ricker pulse was perhaps more useful for validating the pushover response determined from FEM. However, it is noted, and will be further elaborated in the following section, that this pulse would be much more efficient in describing the M–θ behaviour of the large foundation as well, had the pier column been stiffer or rigid enough to supress swaying in favour of rocking.

The centrifuge models were subsequently subjected to further consecutive and identical Ricker pulses, which demonstrated that the foundations could be pushed further into the large rotation range to provide a more complete determination/validation of the pushover response, as shown in Figure 12 (note the change in scales compared with Figure 11). In the case of the large foundation (Figure 12(a)), the point of peak moment and rotation in the positive quadrant (shown by a circular marker) tracks laterally to the right along the backbone curve, confirming that the foundation is moving into the elasto-plastic plateau, while for the small foundation the successive pulses capture the descending branch of the backbone curve, although the moment capacity appears to be slightly higher than that predicted from the FEM. Although not tested here, a smaller magnitude pulse (or pulses) could first have been used with both foundations to determine a point (or multiple points) on the initial elastic section of the backbone curve.

The results shown in Figure 12 suggest that the use of multiple sequential Ricker pulses allows the virtual pushover to be conducted to a desired amount of rotation. The maximum moment points can then be joined together to provide a good estimate of the backbone curve (or, preferentially, to validate an independent calculation, e.g. by FEM).

6. Simplified analytical methodology

Following validation of the new procedure, it was considered desirable to develop a simple analytical methodology to allow estimation of the characteristics of the Ricker pulse (f_E, PGA) required to describe the monotonic pushover response of similar single-degree-of-freedom equivalent oscillator systems having height to centre of mass = H and contact width with the soil = B for use in experimental modelling without the need to use preliminary numerical analysis. To do so, it was necessary to make the simplification of considering the pier as

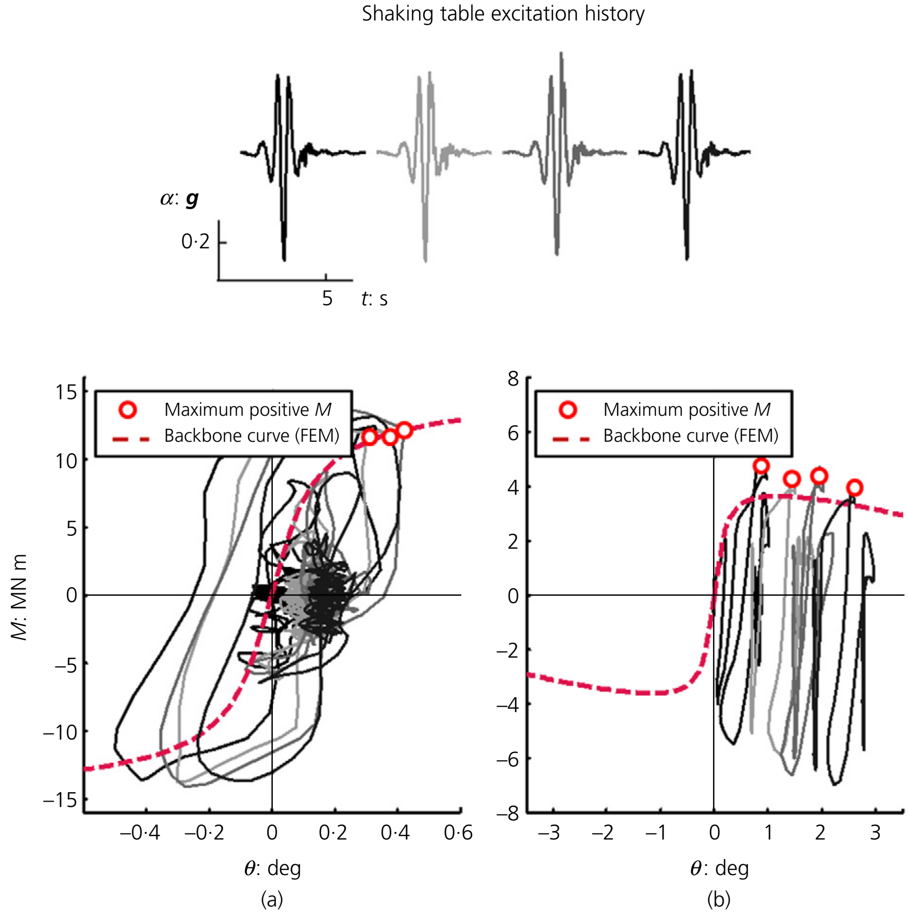

Figure 12. Foundation moment–rotation loops recorded for a series of four successive, practically identical, Ricker pulses (f_E = 1 Hz, PGA = 0·6***g***), compared with monotonic FE predictions: (a) large foundation and (b) small foundation

rigid enough to respond predominantly through rocking and minimise flexural deformation of the column. This would be a valid assumption in the case of a relatively slender pier ($H/B >$ 1·5) supported on a shallow foundation designed according to the principle of rocking isolation (see Gelagoti *et al*., 2012; Loli *et al*., 2014). In a few words, this refers to an under-designed foundation (with $FS_E < 1$) and a moment capacity lower than the capacity of the supported column section.

A series of further numerical analyses was conducted, including all the aforementioned Ricker pulses (Figure 3) for the same numerical model, with the only difference being the stiffness of the column, which was 100 times larger than in the centrifuge tests, so as to be close to rigid. The results are summarised in Figure 13 for both foundation sizes. For PGA > $B/(2H)$ – that is, when uplifting is expected – the maximum rotation experienced by the foundations was found to have a very strong correlation with the spectral displacement of the free-field motion at large periods (here a period of 5 s was taken as reference). More specifically, the following relationship may be deduced

3. $$\sin(\max(\theta)) = S_d^{T=5s}/H \quad \text{for} \quad \theta_{\text{uplift}} > \theta > \theta_c$$

Knowing the desired maximum foundation rotation, one may use Equation 3 to determine the spectral displacement required and hence the characteristics of a suitable pulse. It should be noted that this methodology is valid in the large displacement domain, where the foundation response is outside of the linear regime and uplifting or soil yielding takes place. This is to say, the desired maximum rotation may be a fraction of the critical rotation causing overturning on a rigid base, $\theta_c = \text{a}\tan(B/(2H))$, and presumably greater than the rotation causing onset of uplifting (θ_{uplift}). The latter may be approximated making use

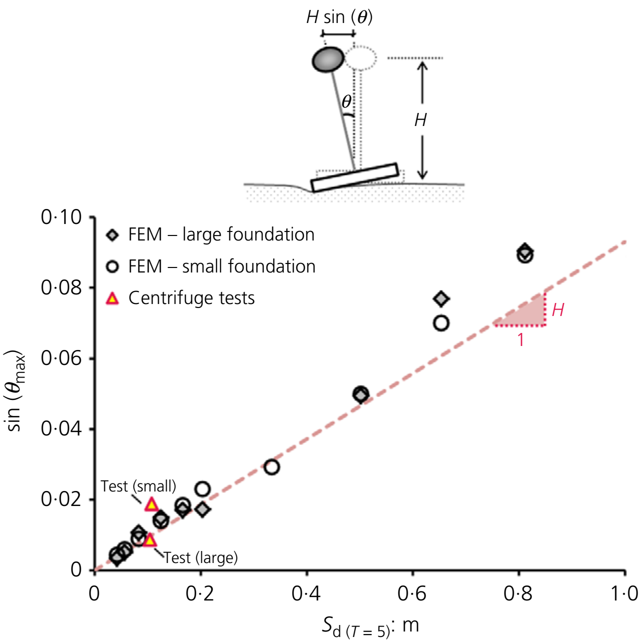

Figure 13. Summary of numerical and experimental results: maximum drift experienced at the deck due to foundation rotation $\delta_{R,max} = H\sin(\theta_{max})$, with respect to the large period spectral displacement $S_{d(T=5\,s)}$ of the free-field excitation

of the Winkler foundation model as described by Apostolou *et al.* (2007).

7. Summary and conclusions

In this paper it has been demonstrated that a Ricker wavelet-type ground motion can be used in a centrifuge EQS to determine or validate the pushover response of shallow foundation systems, without requiring additional actuator set-ups. This approach was found to provide useful information on the foundation response for cases when either small or large amounts of rocking are expected. A structure representing a typical bridge pier tested with two different sizes of shallow foundation was considered, with 3D non-linear dynamic FE modelling used initially to demonstrate the concept and define the characteristics of the Ricker pulses. Centrifuge testing was then conducted which demonstrated that the shape of the 'backbone' moment–rotation curve for the foundations could be determined to be enveloping the moment–rotation response from an appropriately sized Ricker pulse, and that this matched the prediction from the FE modelling. It was further shown that the subsequent application of additional pulses could extend the curve to larger rotations. A simple expression was also developed, based on the centrifuge test data and further numerical parametric study that can be used in determining the properties of the Ricker pulse that will produce a desired amount of rotation for systems with different aspect ratios (*H*/*B*). It is expected that the use of Ricker pulses will be particularly useful in characterising system response in future centrifuge tests of seismic soil–structure interaction problems, particularly given the current trend towards novel foundation designs that use foundation rocking to isolate the structure seismically for which determination of the pushover response is extremely important.

8. Limitations

The presented methodology has been developed on the basis of centrifuge testing and numerical analysis of single-degree-of-freedom structures supported on shallow footings and its implementation naturally refers to such structures. The method relies on the seismically induced rocking vibration of the structure and therefore its effectiveness depends on the ability of the structure to respond predominantly through rocking as opposed to sliding or flexural vibrations. This requirement is related to the geometry (slenderness) and the rigidity of the structure. In particular, the method was shown to provide accurate results for slender structures ($H/B > 1{\cdot}5$) with foundations designed in accordance with the newly introduced concept of rocking isolation.

Acknowledgements

The first author acknowledges the financial support from the project FORENSEIS, financed through the ARISTEIA programme of the Ministry of Education of Greece, and the Coordinator of this project, Professor George Gazetas, whose mentoring and ideas are greatly appreciated. The authors also thank Mark Truswell for his assistance with the centrifuge tests and model fabrication.

REFERENCES

Al-Defae AH and Knappett JA (2014a) Stiffness matching of model reinforced concrete for centrifuge modelling of soil–structure interaction. In *Proceedings of the 8th International Conference on Physical Modelling in Geotechnics, ICPMG'14, Perth, Australia, 14–17 January* (Gaudin C and White D (eds)). CRC Press, London, UK, pp. 1067–1072.

Al-Defae AH and Knappett JA (2014b) Centrifuge modelling of the seismic performance of pile-reinforced slopes. *Journal of Geotechnical and Geoenvironmental Engineering, ASCE* **140(6)**: 04014014.

Al-Defae AH, Caucis K and Knappett JA (2013) Aftershocks and the whole-life seismic performance of granular slopes. *Géotechnique* **63(14)**: 1230–1244.

Anastasopoulos I, Gazetas G, Loli M, Apostolou M and Gerolymos N (2010) Soil failure can be used for seismic protection of structures. *Bulletin of Earthquake Engineering* **8(2)**: 309–326.

Anastasopoulos I, Gelagoti F, Kourkoulis R and Gazetas G (2011) Simplified constitutive model for simulation of cyclic response of shallow foundations: validation against laboratory tests. *Journal of Geotechnical and Geoenvironmental Engineering, ASCE* **137(12)**: 1168–1154.

Apostolou M, Gazetas G and Garini E (2007) Seismic response of slender rigid structures with foundation uplifting. *Soil Dynamics and Earthquake Engineering* **27(7)**: 642–654.

Bertalot D (2012) *Behaviour of Shallow Foundations on Layered Soil Deposits Containing Loose Saturated Sands During Earthquakes*. PhD thesis, University of Dundee, UK.

Bertalot D, Brennan AJ, Knappett JA, Muir Wood D and Villalobos FA (2012) Use of centrifuge modelling to improve lessons learned from earthquake case histories. In *Proceedings of the 2nd European Conference on Physical Modelling in Geotechnics, Eurofuge 2012, 23–24 April, Delft, the Netherlands*. Delft University of Technology and Deltares, Delft, the Netherlands.

Brennan AJ, Knappett JA, Bertalot D *et al.* (2014) Dynamic centrifuge modelling facilities at the University of Dundee and their application to studying seismic case histories. In *Proceedings of the 8th International Conference on Physical Modelling in Geotechnics, ICPMG'14, Perth, Australia, 14–17 January* (Gaudin C and White D (eds)). CRC Press, London, UK, pp. 227–233.

Butterfield R and Gottardi G (1994) A complete three dimensional failure envelope for shallow footings on sand. *Geotechnique* **44(1)**: 181–184.

CEN (Comité Européen de Normalisation) (2004) EN 1998-1:2004: Eurocode 8: Design of structures for earthquake resistance – Part 1: general rules, seismic actions and rules for buildings. Comité Européen de Normalisation, Brussels, Belgium.

CEN (2005) EN 1992-2:2005: Eurocode 2: Design of concrete structures — Part 2: concrete bridges. Design and detailing rules. Comité Européen de Normalisation, Brussels, Belgium.

Gajan S and Kutter BL (2008) Capacity, settlement, and energy dissipation of shallow footings subjected to rocking. *Journal of Geotechnical and Geoenvironmental Engineering, ASCE,* **134(8)**: 1129–1141.

Gajan S, Kutter BL, Phalen JD, Hutchinson TC and Martin G (2005) Centrifuge modeling of load–deformation behavior of rocking shallow foundations. *Soil Dynamics and Earthquake Engineering* **25(7–10)**: 773–783.

Gelagoti F, Kourkoulis R, Anastasopoulos I and Gazetas G (2012) Rocking isolation of frame structures founded on separate footings. *Earthquake Engineering & Structural Dynamics* **41(7)**: 1177–1197.

Knappett JA, Reid C, Skeffington K, O'Reilly K and Gilhooley P (2010) Modelling precast concrete piling for use in the geotechnical centrifuge. In *Proceedings of the 7th International Conference on Physical Modelling in Geotechnics, ICPMG'10, Zürich* (Springman S, Laue J and Seward L (eds)). CRC Press, London, UK, pp. 141–146.

Knappett JA, Reid C, Kinmond S and O'Reilly K (2011) Small-scale modelling of reinforced concrete structural elements for use in a geotechnical centrifuge. *Journal of Structural Engineering, ASCE* **137(7)**: 1263–1271.

Loli M, Knappett JA, Brown MJ, Anastasopoulos I and Gazetas G (2014) Centrifuge modeling of rocking – isolated inelastic RC bridge piers. *Earthquake Engineering & Structural Dynamics* **43(15)**: 2341–2359.

Paolucci R, Shirato M and Yilmaz MT (2007) Seismic behavior of shallow foundations: shaking table experiments vs numerical modeling. *Earthquake Engineering and Structural Dynamics* **37(4)**: 577–595.

Pecker A (2005) Design and construction of the foundations of the rion antirion bridge. In *Proceedings of the 1st Greece–Japan Workshop on Seismic Design, Observation and Retrofit of Foundations* (Gazetas G, Goto Y and Tazoh T (eds)). National Technical University of Athens, Athens, Greece, pp. 119–130.